



Electrical selection for planktonic sludge microbial community function and assembly

Aijie Wang^{a,b,*}, Ke Shi^a, Daliang Ning^c, Haoyi Cheng^{a,b}, Hongcheng Wang^{a,b}, Wenzong Liu^{a,b}, Shuhong Gao^{a,b}, Zhiling Li^a, Jinglong Han^{a,b}, Bin Liang^{a,b,*}, Jizhong Zhou^c

^a State Key Laboratory of Urban Water Resource and Environment, School of Environment, Harbin Institute of Technology, Harbin 150090, China

^b State Key Laboratory of Urban Water Resource and Environment, School of Civil and Environmental Engineering, Harbin Institute of Technology Shenzhen, Shenzhen 518055, China

^c Institute for Environmental Genomics, Department of Microbiology and Plant Biology, University of Oklahoma, Norman, OK 73019, USA

ARTICLE INFO

Keywords:

Hydrolysis acidification (HA)
Electroselection
Planktonic sludge microbial community
Azo dye biotransformation
Microbial interaction
Microbial community assembly

ABSTRACT

Electrostimulated hydrolysis acidification (eHA) has been used as an efficient biological pre-treatment of refractory industrial wastewater. However, the effects of electrostimulation on the function and assembly of planktonic anaerobic sludge microbial communities are poorly understood. Using 16S rRNA gene and metagenomic sequencing, we investigated planktonic sludge microbial community structure, composition, function, assembly, and microbial interactions in response to electrostimulation. Compared with a conventional hydrolysis acidification (HA) reactor, the planktonic sludge microbial communities selected by electrostimulation promoted biotransformation of the azo dye Alizarin Yellow R. The taxonomic and functional structure and composition were significantly shifted upon electrostimulation with azo dyes degraders (e.g. *Acinetobacter* and *Dechloromonas*) and electroactive bacteria (e.g. *Pseudomonas*) being enriched. More microbial interactions between fermenters and decolorizing and electroactive bacteria, as well as fewer interactions between different fermenters evolved in the eHA microbial communities. Moreover, the decolorizing bacteria were linked to the higher abundance of genes encoding for azo- and nitro-reductases and redox mediator (e.g. ubiquinone) biosynthesis involved in the transformation of azo dye. Microbial community assembly was more driven by deterministic processes upon electrostimulation. This study offers new insights into the effects of electrostimulation on planktonic sludge microbial community function and assembly, and provides a promising strategy for the manipulation of anaerobic sludge microbiomes in HA engineering systems.

1. Introduction

Hydrolysis acidification (HA) has been widely used as a biological pre-treatment of refractory industrial wastewater to transform macromolecular organic compounds into bioavailable organics for improved biodegradability (Chen et al., 2020; Guerrero et al., 1999; Wang et al., 2014). However, numerous toxic and hazardous organic contaminants derived from industrial production and discharges could inhibit the metabolic activity of hydrolytic and acidifying bacteria (Bai et al., 2021; He et al., 2020; Luo et al., 2016). In particular, refractory organic nitrogen contaminants (e.g. nitro-aromatics and azo dyes), with the low electron cloud density of the benzene ring and large steric hindrance formed by nitrogen coupling, have resulted in limited decomposition

and ammonization (NH₄⁺ release) efficiency via the traditional hydrolysis and acidification process (Cohen and Wang, 2002). Using conventional anaerobic biotechnology to efficiently remove organic nitrogen contaminants and total nitrogen is a great challenge. It is also very difficult to upgrade wastewater treatment plants (WWTPs) to meet more stringent discharge standards (Katritzky et al., 2010).

Electrostimulation, the supplying of extra reductive energy (electrode as non-exhaustible electron donor) to anaerobic microorganisms through direct external voltage (< 1.0 V) input for overcoming the energetic barrier, has been thoroughly proven to accelerate the detoxification and degradation of various refractory organic nitrogen contaminants (Chen et al., 2019b; Kong et al., 2015; Liang et al., 2013; Liang et al., 2019; Lin et al., 2019; Wang et al., 2011). Electrostimulated

* Corresponding authors at: State Key Laboratory of Urban Water Resource and Environment, School of Environment, Harbin Institute of Technology, Harbin 150090, China.

E-mail addresses: waj0578@hit.edu.cn (A. Wang), liangbin1214@hit.edu.cn (B. Liang).

<https://doi.org/10.1016/j.watres.2021.117744>

Received 25 June 2021; Received in revised form 27 September 2021; Accepted 3 October 2021

Available online 8 October 2021

0043-1354/© 2021 Elsevier Ltd. All rights reserved.

hydrolysis acidification (eHA) has resulted in a breakthrough in the enhancement of the metabolic activity of functional bacteria participating in hydrolysis-acidification and the biodegradation efficiency of refractory organic pollutants (Cui et al., 2014; Cui et al., 2016a; Cui et al., 2016b; Wang et al., 2016). Our previous studies have created an engineered electrode module (EEM) and a power management system, and subsequently established a construction engineering standard for EEMs that could be assembled on-site for immediate use (Wang et al., 2020a; Wang et al., 2017). The applicable EEM provides a viable and clear path to facilitate the transition between the success of laboratory-based studies and real-world application of the proposed eHA technology to enhance detoxification and decomposition of refractory organics and improve wastewater bioavailability (Wang et al., 2020a).

Numerous studies have focused on examining the microbial community structure and function of electrode biofilms due to the unique ability of extracellular electron transfer by bacteria able to colonize the surfaces of electrodes (Du et al., 2018; Hirose et al., 2018; Yanuka-Golub et al., 2021; Yu et al., 2020; Zhou et al., 2013). In the eHA system for pollutant biotransformation, electrostimulation can make significant impacts on the composition, structure, and function of the electrode biofilm and planktonic sludge microbial communities (Chen et al., 2019a; Jiang et al., 2018; Xu et al., 2016; Zhao et al., 2019). Compared with the limited electrode biofilm, planktonic sludge plays a more significant role in the removal of various pollutants due to the higher biomass and overall metabolic activity (De Vrieze et al. 2018; Park et al., 2020). However, the response of planktonic sludge microbial communities to electrostimulation are poorly understood.

Here, we propose a new concept of “electrical selection”, with the aim to directionally regulate the niche and function of the planktonic sludge microbial communities in HA systems during wastewater treatment. We hypothesize that (i) planktonic sludge microbial community structure and microbial interactions would be significantly altered with electrostimulation; (ii) the electrostimulation-selected planktonic sludge communities would greatly promote the biotransformation of refractory organic nitrogen contaminants (e.g. azo dye), and (iii) planktonic sludge microbial community assembly would be dominated by deterministic process under electrostimulation. Such information is important to provide a basis for the targeted manipulation of anaerobic sludge microbiomes in wastewater treatment engineering systems.

2. Materials and methods

2.1. Reactor construction

A single chamber reactor made of polymethyl methacrylate was constructed (Fig. S1). The working volume was approximately 200 mL with an inner diameter of 7.5 cm and a height of 7 cm. Both the anode and cathode were manufactured using a stainless-steel mesh, which were pretreated according to previously published protocols (Wang et al., 2017). During the experiment, a weak voltage of 0.5 V was supplied by a DC power (FDPS-180, Fudan Tianxin Scientific and Educational Instruments Co., Ltd, Shanghai, China), and a saturated calomel electrode (SCE, + 0.247 V vs. standard hydrogen electrode, SHE) was used as a reference electrode to record the cathode potential. For the control group, the same electrodes, but without power supplement, were installed in the reactors.

2.2. Inoculation and operation

Activated sludge derived from Wenchang municipal wastewater treatment plant (Harbin, China) was used as inoculum. The sludge was added to each reactor and adjusted the mixed liquor suspended solids was 6.0 g/L. Synthetic wastewater containing sewage collected from a local residential area and 100 mg/L azo dye Alizarin Yellow R (AYR) was used as influent. Each reactor was equipped with a magnetic rotor

placed on a six-position magnetic stirrer (84-1, Shanghai Meiyongpu Instru. Co., Ltd., China) at 200 rpm to maintain thorough mixing of the reactor contents. The supernatant was discharged and replaced by fresh medium after AYR was completely transformed and decolorized. The influent was flushed with pure nitrogen (purity > 99.99%) to remove dissolved oxygen. Three different operational modes were conducted, (i) anaerobic reactor without supplying DC power, denoted as HA, (ii) anaerobic reactor with DC power supplied as a closed-circuit, denoted as eHA, and (iii) anaerobic reactor where DC power was temporarily removed (the circuit disconnected for 12 h and remained open when AYR removal efficiency was determined), denoted as eHA-O. Each operational condition was run in three parallel reactors and for at least three repetitions.

2.3. Chemical analysis

Samples taken from the bioreactors were centrifuged at 5000 rpm for 5 min. The supernatant was then filtered through a 0.22 μm filter (Tianjin Jinteng Experiment Equipment Co., Ltd., China) and the collected cells were returned to the corresponding reactor. AYR concentration was determined using a UV-vis spectrophotometer (UV-1800, Shanghai Meipuda instrument Co., Ltd., China) at 374 nm. Its transformation products, *p*-phenylenediamine (PPD) and 5-aminosalicylic acid (5-ASA), were quantified using an ultra-performance liquid chromatography (UPLC, Agilent 1290, Agilent Co., Ltd., USA) equipped with a UV detector at 288 nm and a C18 column (2.1 \times 100 mm, Waters Co., USA). The mobile phase was ultrapure water with 0.1% formic acid and methanol (9:1, V/V) at a flow rate 0.2 mL/min. The AYR degradation rates were fitted using pseudo-first-order kinetic reaction and its degradation efficiency (DE) was calculated as previously reported (Cui et al., 2016b). Volatile fatty acid (VFA) and biogas were analyzed by a gas chromatograph (7890A GC system, Agilent Co., Ltd., USA) equipped with FID (flame ionization detector) and TCD (thermal conductivity detector) detectors as previously described (He et al., 2021).

2.4. DNA extraction and microbial community analysis

Planktonic sludge was sampled when the reactor was stirring to obtain a homogenous microbial sample after the bioreactor start-up (day 30, designated as HA-1 for control group and eHA-1 for the electrostimulation group) and during stable operation (day 100, designated as HA-2 for control group and eHA-2 for the electrostimulation group). Nine samples were collected from three biologically replicated reactors.

Sludge DNA was extracted following the method previously described (Zhou et al., 1996). The V4 region of the 16S rRNA genes were amplified using primers 515F and 806R and subsequently sequenced on the Illumina MiSeq platform (Illumina, San Diego, USA) by Majorbio Bio-pharm Technology Co., Ltd. (Shanghai, China). Operational taxonomic units (OTUs) were generated by UPARSE at 97% identity and sequencing results were analyzed utilizing an online platform (www.majorbio.com). Metagenomic sequencing was performed to determine the relative abundance of functional genes and analyzed according to previous protocols (Bai et al., 2021). The raw 16S rRNA genes and metagenomic reads have been deposited into the NCBI Sequence Read Archive (SRA) database (Accession number: PRJNA704102).

2.5. Statistical analysis

The difference of bioreactor performance between electrostimulation and control groups was calculated by two-paired Student's *t*-test. The ordination pattern of the sludge microbial communities in the eHA and HA systems were determined by Principal co-ordinates analysis (PCoA) based on Bray-Curtis distance. Three complementary non-parametric multivariate analysis of variance (Adonis), analysis of similarity (ANOSIM), and multi-response permutation procedure (MRPP) based on Jaccard and Bray-Curtis distances were performed to test the

dissimilarities in the planktonic sludge microbial community composition and structure under different operational modes. Redundancy analysis (RDA) and Spearman's rank correlation analysis were conducted to determine the linkage between bioreactors' performances and microbial community composition. The difference of microbial community composition at genus level was performed by the Welch's *t*-test. The phylogenetic molecular ecological networks (pMENS) based on random matrix theory (RMT) were constructed according to a previously published pipeline (Deng et al., 2012; Zhou et al., 2010; Zhou et al., 2011) and the networks were visualized with Gephi 0.9.2 software. Infer Community Assembly Mechanisms by Phylogenetic-bin-based null model analysis (iCAMP) (Ning et al., 2020) was used to quantitate the planktonic sludge microbial community assembly in response to electrostimulation and the standardized effect size (Cohen's *d*) was calculated to assess the effect of electrostimulation on ecological processes ($|d| > 0.8$ defined as large effect size, $0.5 < |d| \leq 0.8$ defined as medium effect size, $0.2 < |d| \leq 0.5$ defined as small effect size and $|d| \leq 0.2$ defined as negligible effect size). Normalized stochasticity ratio (NST) (Ning et al., 2019) and neutral species percentage (NP) (Burns et al., 2016; Sloan et al., 2010) were also applied to the dataset. The significance of the difference in relative importance of ecological process between electrostimulation and control groups was analyzed based on permutation *t*-test (1000 times).

3. Results and discussion

3.1. AYR transformation performance under different operational modes

After 30 days of stable current generation, an indication of successful eHA start-up, AYR degradation efficiency was determined (Fig. 1a). For eHA, the AYR degradation efficiency at 8 h (DE_{8h}) reached $91.94 \pm 1.49\%$ and was $89.97 \pm 0.94\%$ when electricity was temporarily

removed (eHA-O). Meanwhile, the AYR degradation efficiency for HA was $84.57 \pm 2.98\%$. The AYR degradation data was fitted with pseudo-first-order kinetics and the rate constant of eHA-O was significantly ($P < 0.01$) higher than HA (Fig. 1b). After the bioreactors were steadily operated for 100 days, the AYR degradation efficiency tendency was consistent with the former stage (Fig. 1c). DE_{8h} of eHA was $94.62 \pm 2.73\%$, 12.60% higher than that of HA ($82.02 \pm 3.37\%$). DE_{8h} was $91.67 \pm 2.59\%$ for eHA-O, which was 9.65% higher than that of HA. The rate constant of eHA-O was also significantly higher than that of the HA ($P < 0.01$).

To confirm AYR transformation was the cleavage of the azo bond rather than adsorption, the AYR reduction products were also determined (Fig. S2a, b). The anaerobic AYR transformation pathway has been previously investigated (Cui et al., 2014), and PPD and 5-ASA were found to be formed by the cleavage of the azo bond. PPD concentration increased with AYR transformation, and the recovery efficiency was more than 70% after 6 h. The relatively low recovery efficiency during the first 4 h may be derived from the adsorption of AYR to sludge instead of biotransformation. Accordingly, the DE_{6h} and DE_{8h} (AYR degradation efficiency at 6 h and 8 h) was selected to evaluate the performance of the different operational modes. AYR transformation efficiency was significantly improved under electrostimulation and the order was eHA > eHA-O > HA.

The major VFAs were acetic acid and propionic acid under the different operational modes (Fig. S2c). The lower VFA concentrations during eHA mode indicated that exoelectrogens on the anode are potentially consuming the organic acid for current generation, which was the driving force improving AYR biotransformation at the cathode. The results also corresponded with lower methane production (0.079 mmol/d for HA and 0.031 mmol/d for eHA) and higher AYR transformation efficiency. Therefore, electrostimulation may alter the electron transfer pathway within planktonic sludge microbial communities.

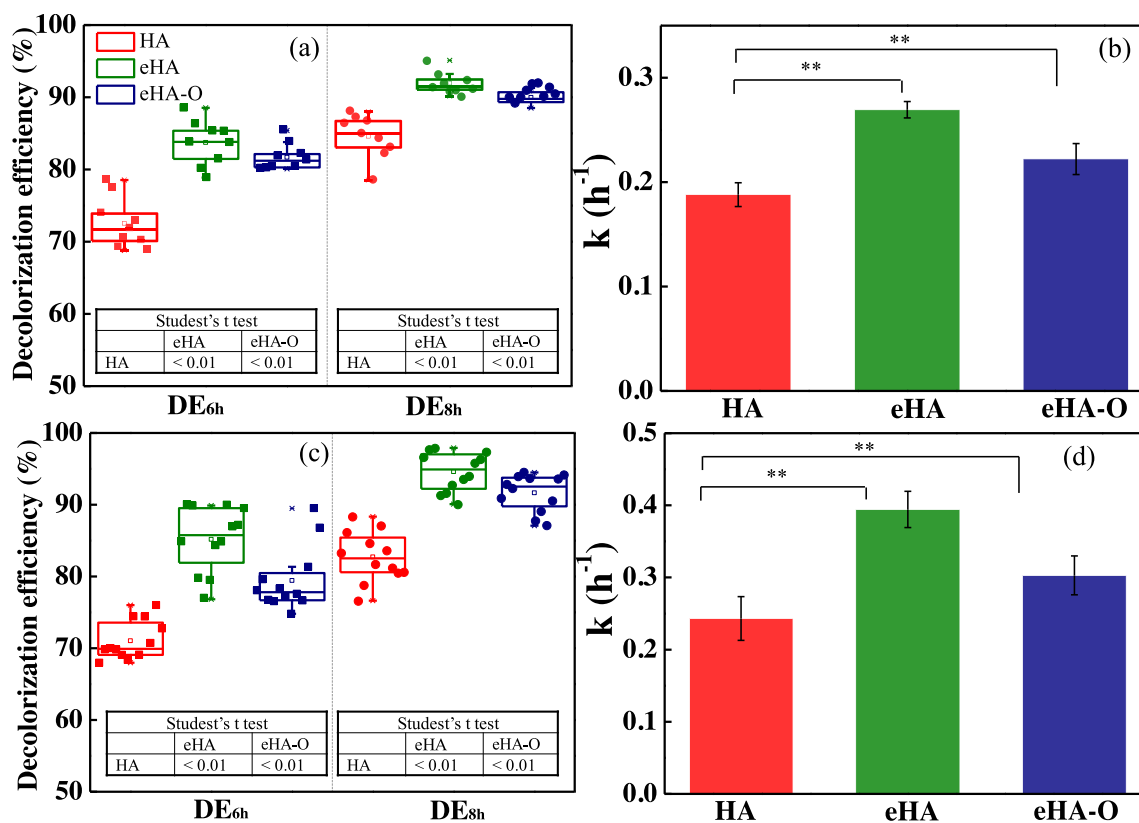


Fig. 1.. Effects of electrostimulation on azo dye degradation efficiencies. Degradation efficiency (DE) and rate constant (*k*) on day 30 (a, b) and day 100 (c, d) (** denotes Student's *t*-test, $P < 0.01$).

During eHA-O mode, the accumulated VFAs concentration was lower than HA, which may be derived from a greater number of cooperative relationships between fermenters and decolorizer after electrostimulation. However, during HA mode, the complex organics were fermented to VFAs by fermentative bacteria, and the additional acetic acid was further utilized to produce methane.

The superior pollutant removal efficiency after supplying with external power has been widely recognized due to the combined contribution of electrochemical reduction and biological reduction (Cui et al., 2016b; Dan et al., 2012; Jiang et al., 2018; Wang et al., 2016). Interestingly, AYR degradation efficiency was still higher than that of HA when the external power was temporarily removed. The degradation efficiency at day 100 was also significantly higher than day 30 ($P < 0.01$) regardless of the operational modes (Fig. S2 d, e). Although previous research has documented that anodic electroactive biofilms can store charge in self-produced redox proteins, with a discharge time of 60 s (Zhang et al., 2018) or intermittent power supply (Wang et al., 2020b). In our experiment, the higher AYR transformation efficiency was determined when the circuit was kept open after having been disconnected for 12 h, and the planktonic sludge may play a more important role in AYR transformation due to its larger biomass. These results implied that the distinct planktonic sludge microbial community composition and interactions of the eHA group contributed to the improved functional performance.

3.2. Shifts in planktonic sludge microbial communities

To examine the effects of electrostimulation on the selectivity of functional microbes, planktonic sludge microbial community composition and structure were analyzed using 16S rRNA gene-based Illumina MiSeq sequencing. As indicated by PCoA, based on Bray-Curtis distance matrix, electrostimulation markedly shifted phylogenetic structure of the planktonic sludge microbial communities. HA and eHA groups were well separated from each other, especially after 100 days (Fig. 2a). Additionally, three complementary non-parametric multivariate statistical tests (MRPP, ANOSIM, and Adonis), calculated with Bray-Curtis and Jaccard distances, further indicated that the planktonic sludge microbial community structure was substantially different ($P < 0.05$) between the HA and eHA groups on day 30, and the difference became more significant as time proceeded ($P < 0.01$, on day 100) (Table 1). These results indicated that the composition and structure of the planktonic sludge microbial communities varied markedly under electrostimulation. To link the shift of microbial communities in the eHA system to bioreactor performance, RDA was performed and showed that microbial community structure (response variables) was significantly

shaped by explanatory variables including DE_{8h} ($P = 0.007$), rate constant (k) ($P = 0.001$), the accumulated concentration of VFAs ($P < 0.01$), CH_4 ($P = 0.036$), and cathode potential ($P = 0.016$) (Fig. 2b). Overall, explanatory variables related to AYR transformation efficiency were significantly and positively correlated with the microbial community structure within the eHA group, and those related to the accumulated concentration of VFAs were significantly negative correlated. However, the relationships between measured bioreactor performance and the microbial community structure within the HA group were the opposite.

To detect the difference between the potential functional populations within HA and eHA, dissimilarity analyses were conducted based on the Welch's t -test at the genus level (Fig. 3). The dominant genera are usually regarded as functionally significant populations within a microbial community. *Acinetobacter* had the highest relative abundance and significantly enriched under electrostimulation, which was positively correlated with azo dye reduction ($r = 0.39$, $P < 0.05$, Fig. S5). In addition, a previous study reported *Acinetobacter* could utilize acetate as a substrate to transform azo dye (Kong et al., 2018). *Dechloromonas*, which was enriched in eHA, has also been reported to transform azo dye (Long et al., 2019). *Geobacter*, *Desulfovibrio*, and *Desulfobulbus* were enriched after 100 days. Additionally, the relative abundance of *Geobacter* and *Desulfobulbus* were positively correlated with azo dye reduction rate ($r = 0.35$ – 0.57 , $P < 0.05$, Fig. S5). *Geobacter* is capable of reducing nitro groups and azo bonds except for extracellular electron transfer (Liu et al., 2013; Logan et al., 2019; Xu et al., 2019). *Desulfovibrio* and *Desulfobulbus* are capable of electron transfer and have been associated with azo dye degradation under anaerobic conditions (Miran et al., 2015). The two genera also may take part in SO_4^{2-} reduction because the concentration of SO_4^{2-} in sewage are up to dozens of milligrams per liter and the products S^{2-} could be acted as electron donor for AYR bioreduction (Luo et al., 2019). *Pseudomonas*, a bacterial genus with electroactive members that can secrete mediators such as phenazine, were enriched under electrostimulation on the day 30 ($P < 0.05$). *Pseudomonas* has been shown to be capable of reducing azo dyes and nitroaromatics (Chang et al., 2001). *Pseudomonas* was positively correlated with azo dye reduction rate ($r = 0.45$, $P = 0.006$) and cathode potential ($r = 0.32$, $P = 0.061$) (Fig. S5). The relative abundance of norank_f_Bacteroidetes_vadinHA17, norank_o_Saccharimonadales, and norank_f_Anaerolineaceae were not significantly different between HA and eHA. These genera are able to degrade complex organic compounds under anaerobic or facultative conditions (Shi et al., 2021). The above results suggested that decolorizers were enriched under electrostimulation, while the relative abundance of fermentative bacteria were not significantly different from the control group. Worth noting, the electrode biofilm might indirectly affect the planktonic microbial

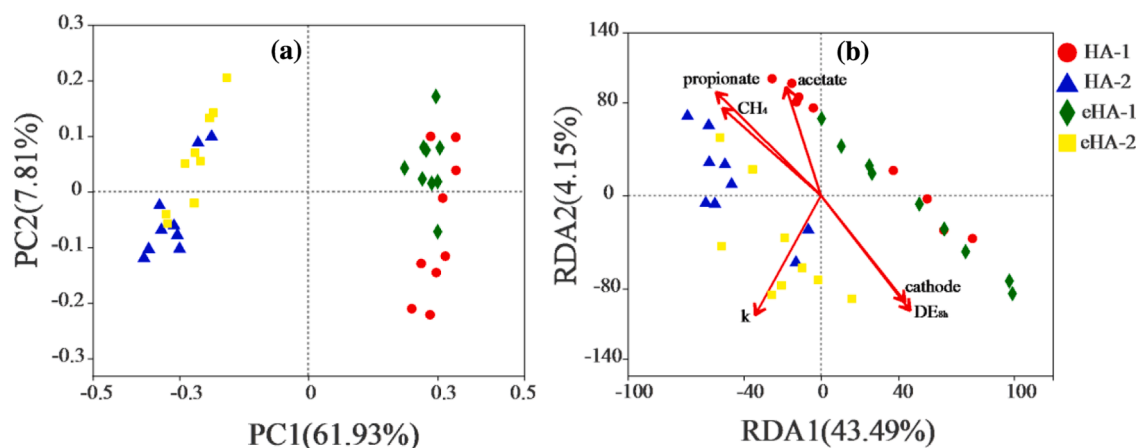


Fig. 2. Effect of electrostimulation on planktonic sludge microbial community structure. (a) Principal co-ordinates analysis (PCoA) based on Bray-Curtis distance of 16S rRNA gene sequences, significance test based on ANOSIM ($r = 0.7417$, $P = 0.001$), and (b) Redundancy analysis (RDA) of 16S rRNA gene sequences data and explanatory variables.

Table 1

Significance tests of the effects of electrostimulation on the overall planktonic sludge microbial community structure with three different statistical approaches (Bold indicates $P < 0.05$).

	Jaccard distance						Bray-Curits distance					
	MRPP		Anosim		Adonis		MRPP		Anosim		Adonis	
	δ	P	R	P	F	P	δ	P	R	P	F	P
HA-1 vs eHA-1	0.420	0.024	0.110	0.039	1.255	0.028	0.249	0.019	0.239	0.020	2.892	0.016
HA-2 vs eHA-2	0.424	0.001	0.328	0.001	1.559	0.001	0.280	0.002	0.389	0.005	4.066	0.002

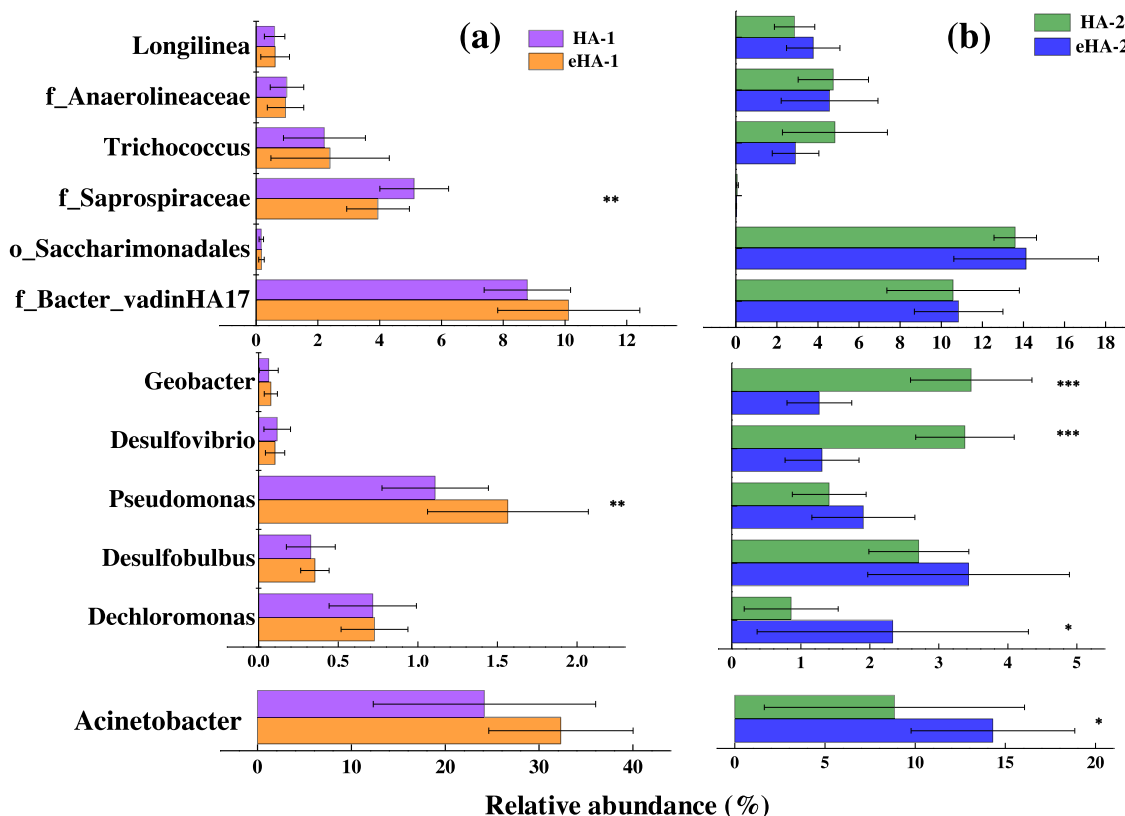


Fig. 3. Effect of electrostimulation on planktonic sludge microbial community composition at the genus level on day 30 (a) and day 100 (b); (*: Welch's t -test, $P < 0.1$, **: $P < 0.05$).

community. Electrostimulation could gather differed core functional groups across electrode and plankton (Cheng et al., 2021; Lin et al., 2019; Wang et al., 2020c). Microorganisms capable of extracellular electron transfer assemble on the anode, pollutant reduction (e.g. dechlorinators and decolorizers) and methane production (e.g. hydrogenotrophic methanogens) on the cathode, organics degradation (e.g. fermenters) and pollutants reduction in the plankton. Also, the detached biofilm might participate in planktonic microbial community alternation.

3.3. Variation of microbial interactions within planktonic sludge communities

Beyond microbial community structure and composition difference, biodiversity includes the complex microbial interactions between different species, and various biological populations interact with each other to conduct special ecological functions (Zhou et al., 2011). Phylogenetic molecular ecological networks (pMEN) are constructed using the random matrix theory (RMT)-based network approach, which is powerful tool for describing microbial associations using high-throughput sequencing data (Feng et al., 2017; Yuan et al., 2021; Zhou et al., 2010; Zhou et al., 2011). On day 30, the HA network consisted of 200 nodes (OTUs) and 539 links (interactions), and for eHA,

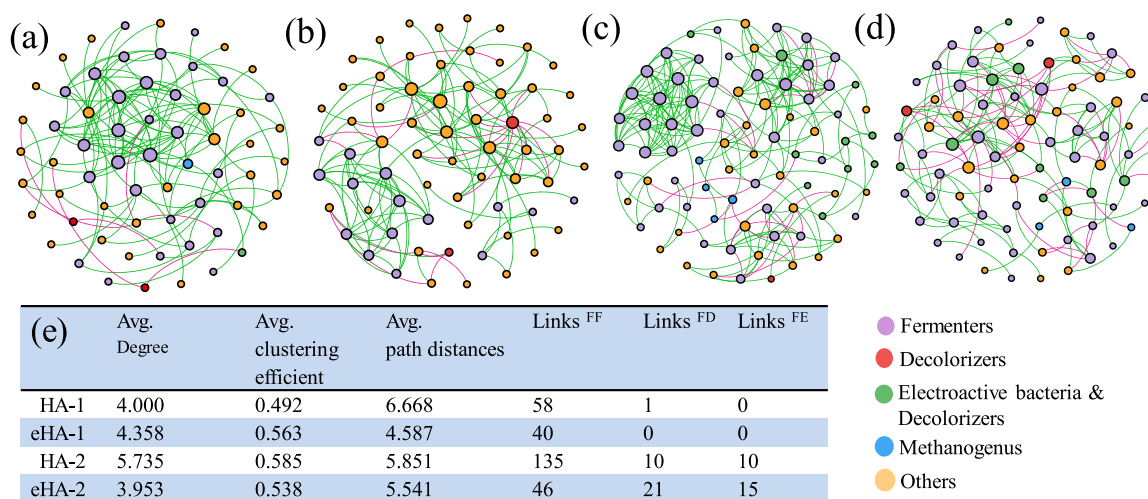
191 nodes and 444 links (Fig. S6). The number of nodes and links decreased after 100 days. The difference of overall network topological properties was compared by calculating several important parameters (Table 2). The average connectivity (avgK), an indicator of network complexity, was 5.39 and 4.65 for HA-1 and eHA-1, 4.76 and 3.57 for HA-2 and eHA-2, respectively. Higher average connectivity indicates a more complex relationship, and lower average clustering coefficient indicates stronger connections. As illustrated, more complicated interactions appeared in HA, and the majority of links (> 70%) in all networks were positive (Fig. S6). The average path distance value was close to the logarithm of the total number of network nodes, meaning that the pMENs had typical small world properties. The modularity (0.639–0.782) was higher than the corresponding randomized networks (0.377–0.504), suggesting the constructed networks were modular. Although the pMENs across different operational stages, with or without electrostimulation, had the typical topological features of many microbial interaction networks (scale-free, small world, and modular architecture), the average path distance, average clustering coefficient, and modularity of HA and eHA networks were significantly different ($P < 0.01$) (Table 2).

Subnetworks were constructed with the keystone microorganisms identified by Z-P plot (Fig. S8) and dominant genera (Fig. 4). For HA-1, this subnetwork consisted of 27.50% of total nodes and 23.93% of total

Table 2.

Topological properties of the empirical pMENs of planktonic sludge microbial communities under electrostimulation and control, and their associated random pMENs.

Datasets	Empirical networks					Random networks ^c		
	Similarity threshold	Avg connectivity (avgK)	Avg path distance	Avg clustering coefficient	Modularity	Avg path distance ± SD	Avg clustering coefficient ±SD	Modularity ±SD
HA-1	0.890	5.390	7.507 ^a	0.336 ^a	0.639 ^a	3.259 ± 0.050	0.068 ± 0.010	0.377 ± 0.007
eHA-1	0.890	4.649	5.468 ^a	0.377 ^a	0.714 ^a	3.496 ± 0.051	0.036 ± 0.009	0.430 ± 0.008
HA-2	0.920	4.764	5.817 ^b	0.452 ^b	0.725 ^b	3.208 ± 0.065	0.069 ± 0.014	0.400 ± 0.009
eHA-2	0.920	3.569	5.612 ^b	0.393 ^b	0.782 ^b	3.775 ± 0.077	0.030 ± 0.011	0.504 ± 0.013

^a Significant difference ($P < 0.001$) between HA-1 and eHA-1 values.^b Significant difference ($P < 0.001$) between HA-2 and eHA-2 values.^c The random networks were generated by rewiring all of the links of a pMEN with the identical numbers of nodes and links to the corresponding empirical pMEN.**Fig. 4.** Subnetworks to visualize interactions among dominant genera and keystone microorganisms of planktonic sludge microbial communities. Green and red lines indicate positive and negative associations, respectively. (a) HA-1, (b) eHA-1, (c) HA-2, (d) eHA-2, and (e) topological properties of the subnetworks and brief summary of link numbers (FF: links among fermenters; FD: links between fermenters and decolorizers; FE: links between fermenters and electroactive bacteria).

links from the original network. There was a connected cluster among the fermentative bacteria in which all links were positive, while the microbial interactions of the nodes related to azo dye reduction (e.g. *Acinetobacter*) and organics fermentation was little (Fig. 4a). For eHA-1, the network size (24.08% of total nodes, whereas covering 33.55% of total links) was similar to HA-1 (Fig. 4b). However, there was a cluster centralized with *Acinetobacter* (a decolorizer). On day 100, networks of the HA and eHA communities consisted of 67.48% of total nodes covering 81.23% of total links and 73.28% of total nodes covering 81.16% of total links, respectively, suggesting that microbial interactions of dominant bacteria and keystones were the majority of all interactions at this stage whether or not electrostimulation was used. However, more complicated interactions (more links) among fermenters and fewer interactions between fermenters and decolorizers were observed in the HA-2 group (Fig. 4c). Electrode biofilm (e.g. electroactive bacteria and decolorizers) detachment was inevitable, which could affect the planktonic microbial interactions (Lin et al., 2019). For the eHA-2 group, fermenters (e.g. norank_o_Saccharimonadales) had more positive relationships with decolorizers (e.g. *Acinetobacter*) and electroactive bacteria (e.g. *Desulfovibrio*) (Fig. 4d). However, there were fewer interactions among fermenters. Collectively, microbial interactions were not conserved between the HA and eHA groups. Although less connectivity was observed in the eHA network, functional OTUs (decolorizers, fermenters, and electroactive bacteria) shared more interactions. Therefore, electrostimulation could optimize the microbial

interactions which synergistically enhance the biotransformation of azo dye AYR.

3.4. Variation of the metabolic potential within planktonic sludge communities

In addition to basic microbial community structure, the metabolic potential of planktonic sludge microbial communities on day 100 was explored through metagenomic sequencing, due to more significant difference of microbial communities between the HA-2 and eHA-2 groups. The original gene-set of each community consisted of more than 40 million clean reads and 6 billion bps. PCoA of the original gene-sets at KEGG Orthology (KO) level was performed. The gene-sets derived from the planktonic sludge communities of HA-2 were well separated from those of eHA-2 (Fig. S9), indicating electrostimulation changed functional gene structure. RDA suggested that the composition of functional genes within the eHA-2 group was significantly positively correlated with azo dye transformation rate ($P = 0.058$) and cathode potential ($P = 0.075$), and negatively correlated with accumulated propionate concentration ($P = 0.003$) (Fig. S9). While the relationships of these explanatory variables and the functional gene structure within the HA-2 group was the opposite.

Azoreductase catalyzes the cleavage of the azo bond (-N=N-) to form colorless aromatic amine (Sarkar et al., 2017). According to KEGG annotation, the azoreductase genes detected in this study are NADH

dependent, which means that oxidizable molecules serve as an electron donor to take part in the azo bond breakdown. The total abundances of azoreductase gene (K01118) and NAD(P)H dehydrogenase genes (K00355, K03809, and K19267) were relatively higher in the electrostimulation microcosms (Fig. 5a). Nitroreductase could catalyze the reduction of nitroaromatics using NAD(P)H as an electron donor (Liang et al., 2014) and the gene encoding for nitroreductase (K10679) was also relatively higher in the electrostimulation microcosms (Fig. 5c). More importantly, *Acinetobacter* and *Dechloromonas* related NAD(P)H dehydrogenase genes (K03809) (3.58 and 3.91 times higher, respectively) as well as *Dechloromonas* related nitroreductase gene (K10679) (7.62 times higher) were significantly ($P < 0.05$) more abundant in the electrostimulation microcosms. Based on the 16S rRNA gene sequencing results, these genera were significantly enriched in the planktonic eHA-2 communities, suggesting that they may be involved in the transformation of azo dye AYR by participating in the synthesis of NAD(P)H dehydrogenase and nitroreductase.

Redox mediators could act as electron shuttles between the extracellular NADH dependent azoreductase and NADH dehydrogenase under anaerobic condition (Sarkar et al., 2017). In particular, genes coding for menaquinone (K01661) and ubiquinone (K03182) biosynthesis were identified with significantly ($P < 0.05$) higher relative abundance in the electrostimulation microcosms with *Dechloromonas* as the major source of these genes (Fig. 5b, d). K01661 sequences assigned to this genus were significantly (4.64 times) more abundant in the electrostimulation microcosms. Other functional genes, taxonomically linked to *Dechloromonas*, coding for redox mediators including riboflavin (K00793) and menaquinone (K03183) biosynthesis were also significantly more abundant in the electrostimulation microcosms at 6.04 and 6.86 times, respectively, although the total abundances of

those genes were not higher in the electrostimulation microcosms. Similarly, genes coding for ubiquinone (K06134 and K03179) and riboflavin (K00793 and K11753) biosynthesis were not significantly higher in the electrostimulation groups, while the genes assigned to *Acinetobacter* were significantly ($P < 0.05$) more abundant in the electrostimulation groups (1.81, 3.87, 2.12, and 2.86 times higher, respectively). These results suggested *Dechloromonas* and *Acinetobacter* also played important roles in electron transfer during the reduction of the azo dye AYR as a previously reported *Acinetobacter* can secrete quinone to facilitate extracellular electron transfer (Wang et al., 2020b). *Pseudomonas* are electroactive bacteria that secrete redox mediators such as quinone (Choi et al., 2008). Sequences related to *Pseudomonas* genes coding for ubiquinone (K03182 and K03179) and menaquinone (K03183) biosynthesis were relatively higher in the electrostimulation groups. Genes coding for K03183 assigned to *Desulfobulbus* were significantly ($P < 0.01$) more abundant, indicating this genus may provide additional mediators to accelerate AYR reduction. Overall, the majority of genes participating in AYR transformation were more often taxonomically assigned to decolorizers and electroactive bacteria, and the relative abundance of these genera were also significantly higher under electrostimulation.

3.5. Stochastic vs. deterministic planktonic microbial community assembly

Dissecting the mechanisms controlling biodiversity and microbial community composition under electrostimulation could provide valuable insights into the importance of various ecological processes to planktonic sludge microbial community assembly (Zhang et al., 2019; Zhou et al. 2017; Zhou et al., 2013).

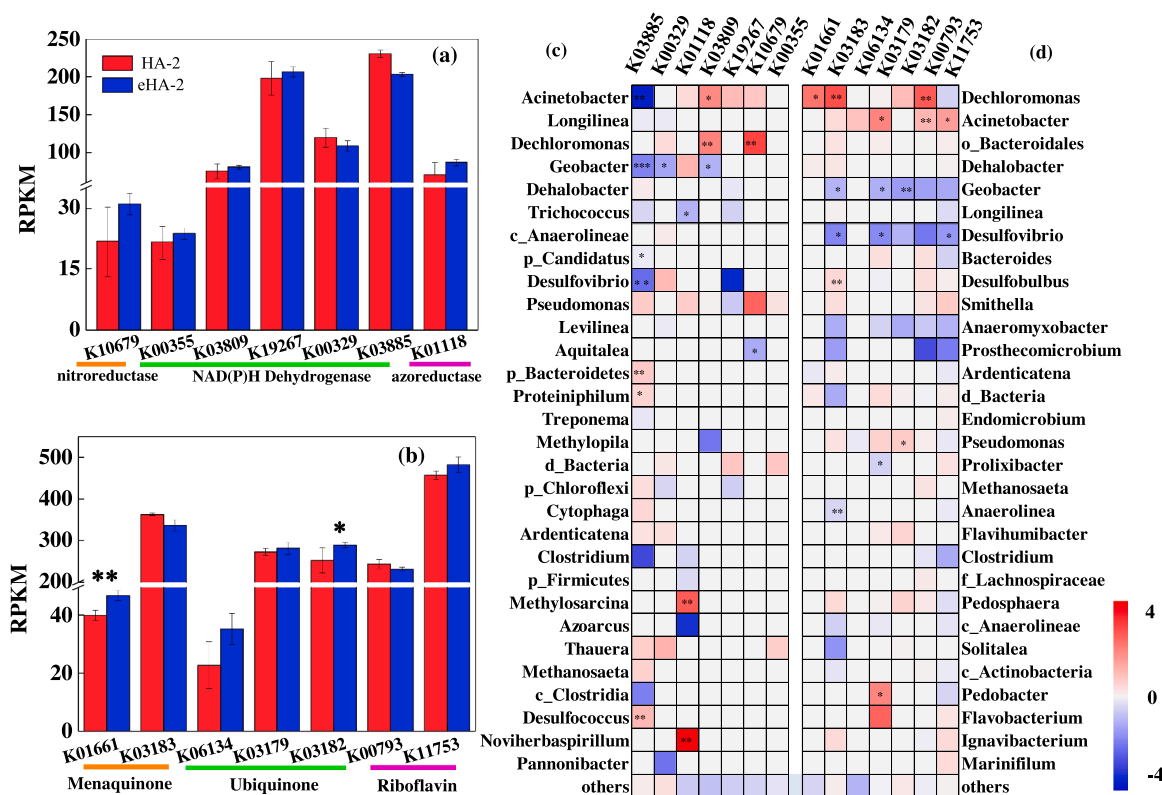


Fig. 5. Effect of electrostimulation on functional genes. (a) Relative abundances of genes encoding for azoreductase (K01118), nitroreductase (K10679), NADH dehydrogenase (K00329 and K03885), NAD(P)H dehydrogenase (K00355, K03809 and K19267), (b) Menaquinone biosynthesis (K01661 and K03183), Ubiquinone biosynthesis (K06134, K03179 and K03182), and Riboflavin biosynthesis (K00793 and K11753) in planktonic sludge microbial communities with electrostimulation (eHA-2 group) or not (HA-2 group) from metagenomic sequencing (*: Student's *t*-test, $P < 0.05$, **: $P < 0.01$ and ***: $P < 0.005$), (c) Heatmap showing the log ratio (\log_2 eHA/HA) of relative abundances of genes coding for nitroreductase and azoreductase, (d) Mediator biosynthesis assigned to microbial community at genus level (top 30 most abundant genera only) in HA-2 and eHA-2 groups. The gray cells indicate data had not been detected.

Firstly, the ecological deterministic process was quantified by abundance-weighted neutral taxa percentage (NP) based neutral-theory model, normalized stochasticity ratios (NST) based on taxonomic (tNST) or phylogenetic metrics (pNST), and iCAMP (Fig. 6a–d). According to NP and NST, the deterministic process contributed an average of 10.31–15.84% and 7.23–18.87% of the community variation for HA-1 and eHA-1, respectively. The estimated deterministic ratio was on average 43.82 and 42.65% based on iCAMP, and the ratio was not significantly different between HA-1 and eHA-1, with negligible effect size (Cohen's $d = 0.17$). But on day 100, tNST and NP revealed that electrostimulation led to a significant ($P < 0.05$) increase of the deterministic ratio. pNST (Cohen's $d = 2.57$) and iCAMP (Cohen's $d = 1.09$) also showed that deterministic process was more important for eHA microbial community assembly with a large effect size. Various approaches indicated that microbial community assembly was more deterministic under electrostimulation over the course of the experiment. Furthermore, the relative importance of different ecological processes including homogeneous selection (HoS), heterogeneous selection (HeS), dispersal limitation (DL), homogenizing dispersal (HD), and drift (DR) was quantified based on iCAMP. In general, the combined fraction of DL, HD, and DR in microbial ecology are considered to be the stochastic processes (Ning et al., 2020). In this study, HoS, DL, and DR were more important in bacterial community assembly, with an average relative importance of 42.60–51.75%, 2.37–11.51%, and 35.65–48.75%, respectively. On day 30, electrostimulation had altered

the relative importance of different processes by only an insignificant amount with medium or small effect size ($|\text{Cohen's } d| = 0.17\text{--}0.73$), but had significantly decreased the importance of dispersal limitation ($P = 0.044$). However, electrostimulation increased the relative importance of homogeneous selection with large effect size (Cohen's $d = -1.09$), and significantly ($P = 0.035$) decreased dispersal limitation with large effect size (Cohen's $d = 2.46$) after 100 d of operation, suggesting the relative importance of the deterministic process increased with the time of electrostimulation.

More importantly, iCAMP can provide useful information on the relative importance of different ecological processes in individual phylogenetic bins or groups (Ning et al., 2020). For this purpose, the 3777 observed OTUs were divided into 69 phylogenetic bins (Fig. 6e and f). After 100 days, homogeneous selection dominated 19 bins (27.53% of bin numbers and 49.86% relative abundance) for the HA-2 group and 22 bins (31.88% of bin numbers and 58.99% relative abundance) for the eHA-2 group (Table. S3). Two of the major bins were Bacteroidetes (Bin 23, 11.32% in total abundance of bins) and Proteobacteria (Bin 65, 21.24% in total abundance of bins). By contrast, drift dominated 23 bins (33.33% of bin numbers and 28.30% relative abundance) and 19 bins (27.54% of bin numbers and 24.45% relative abundance) for HA-2 and eHA-2, respectively, with the most abundant drift-governed bin (Bin 57, 5.67% in total abundance of bins) belonging to the phylum Patescibacteria.

To determine which ecological process was more important for the

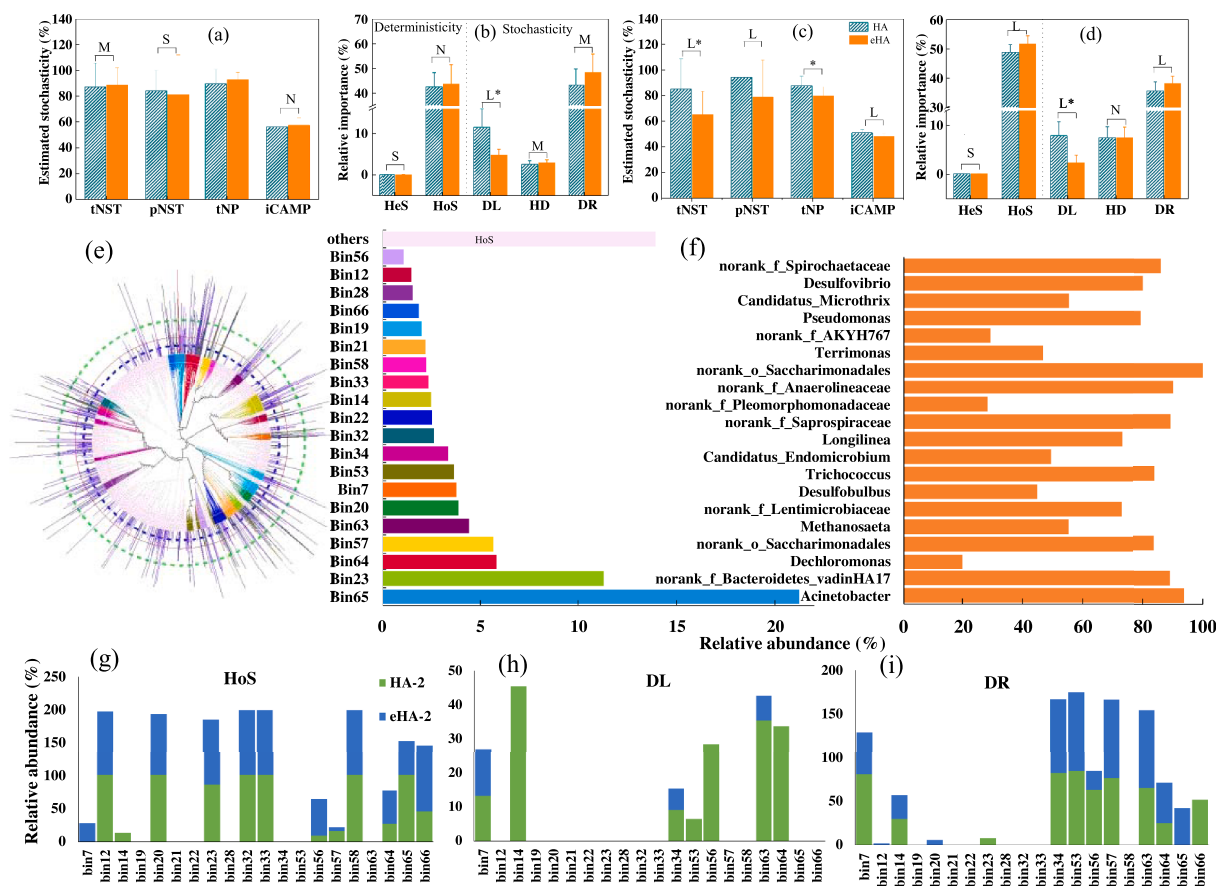


Fig. 6. Relative importance of stochasticity in response to electrostimulation. Stochasticity estimated by different methods at 30 d (a) and 100 d (c). Relative importance of different ecological processes based on iCAMP at 30 d (b) and 100 d (d). Variations of ecological processes across different phylogenetic groups (e–i). Phylogenetic tree (e), relative abundance of each bin (only the top 20 bins were shown in this figure, accounting for a total relative abundance of 86.06%) (left) and the genus with greatest relative abundance in each bin (right) (f). Relative importance of homogeneous selection (g), dispersal limitation (h), and drift (i) in the assembly of the major bins in HA-2 and eHA-2. (One-side significance based on bootstrapping test was expressed as * $P < 0.05$. L, M, S, and N represent large ($|\text{Cohen's } d| > 0.8$), medium ($0.5 < |\text{Cohen's } d| \leq 0.8$), small ($0.2 < |\text{Cohen's } d| \leq 0.5$), and negligible ($|\text{Cohen's } d| \leq 0.2$) effect sizes of electrostimulation, based on Cohen's d (the mean difference between electrostimulation and control divided by pooled standard deviation). HoS: homogeneous selection, HeS: heterogeneous selection, DL: dispersal limitation, HD: homogenizing dispersal, and DR: drift and others).

assembly of dominant genera under electrostimulation, bins containing bacteria contributing to the electrostimulation-induced changes of homogeneous selection, dispersal limitation, and drift on day 100 were further analyzed (Fig 6g and i). The most abundant genus, *Acinetobacter* (88.93% of total abundance in bin 65) was entirely (100%) governed by homogeneous selection within the HA-2 group and mainly (52.89%) dominated by homogeneous selection within the eHA-2 group. *Dechloromonas* (19.94% of bin 64) contributed 22.59% of the electrostimulation-induced increase in homogeneous selection. The two major genera of bin7, *Desulfobulbus* (44.84%) and *Geobacter* (32.43%), were 100% and 70.59% governed by stochastic processes within HA-2 and eHA-2, respectively. *Pseudomonas* (relative abundance of 79.26%) was the most abundant genus of bin 66 and increased the relative importance of homogenous selection under electrostimulation by 54.25%. Based on available metabolic information, the dominant fermenters were norank_f_Bacteroidetes_vadinHA17 (39.40% in total abundance of bin 23) and norank_o_Saccharimonadales (56.03% in total abundance of bin 57). Bin 23 was 85.26% and 100% governed by homogeneous selection for HA-2 and eHA-2, respectively. While bin 57 was 83.85% and 94.26% predominated by stochastic processes for HA-2 and eHA-2, respectively. These results indicated electrostimulation drove the planktonic sludge microbial community assembly to be more deterministic, especially for azo dye degraders and electroactive bacteria.

4. Environmental implications

Undoubtedly, eHA could improve the biotransformation efficiency towards various organic contaminants (Cui et al., 2014; Jiang et al., 2018; Wang et al., 2017). Consequently, it is important to understand how planktonic sludge microbial communities respond to electrostimulation. However, the majority of studies have focused on microbial alpha- and beta-diversity patterns and microbial community composition at the phylum, class, and genus levels for electrode biofilm and planktonic sludge (Chen et al., 2019a; Jiang et al., 2018; Xu et al., 2016). This study demonstrated the significant changes in the planktonic sludge microbial community structure, function, and assembly in response to electrostimulation in a eHA bioreactor.

The directional enrichment of functional microorganisms is the core to ensure the treatment efficiency and functional stability of the

engineering water system. Our results highlighted at least three possible major mechanisms by which the biotransformation efficiency of refractory nitrogen-containing organics could be enhanced by electrostimulation (Fig. 7). The first is through obvious changes in the planktonic sludge microbial community composition and structure. Our findings that significant differences occur in the planktonic sludge microbial communities under electrostimulation is in agreement with studies on electrode biofilm communities that were obviously affected by electrostimulation (Guo et al., 2013; Liao et al., 2018; Lin et al., 2019). Redundancy analysis indicated the shift of functional microbial communities was responsible for more efficient biodegradation of pollutants in eHA. The second is by altered and evolved microbial interactions. Functional redundancy, many coexisting but taxonomically different microorganisms could perform same metabolic functions and the identified taxa encoding each function could vary substantially across time with negligible effect on the function, is common (Louca et al., 2018). Also, microorganisms do not thrive in isolation but in complex associations (Yuan et al., 2021). Phylogenetic microbial ecological networks allow insight into the interactions of different microbial functional populations (Banerjee et al., 2019; Zhou et al., 2011). Our study highlighted that electrostimulation could significantly affect the network structure, and revealed that communities that did not receive electrostimulation had significantly more complex interactions between fermenters. However, more positive interactions of fermenters and decolorizers, as well as fermenters and electroactive bacteria occurred under electrostimulation, which could be responsible for the more efficient functional performance. The last is by enhancing the relative abundance of some functional genes, especially those involved in redox mediator biosynthesis. Mediators play a critical role in indirect extracellular electron transfer (Martinez and Alvarez 2018). These genes were more prevalent in dominant genera such as *Dechloromonas*, *Acinetobacter*, and *Pseudomonas*. More importantly, deterministic assembly played a more significant role in regulating the structure of the eHA planktonic sludge communities, which implies that polarized electrodes could be used as a microbial selector to acclimatize microbial consortia for more efficient functional performance. Accordingly, the introduction of engineered electrode modules (EEM) into HA units would be a practicable manipulation to select functional microorganisms for the efficient biotransformation of various pollutants. Considering the actual operability and energy savings, the planktonic sludge after

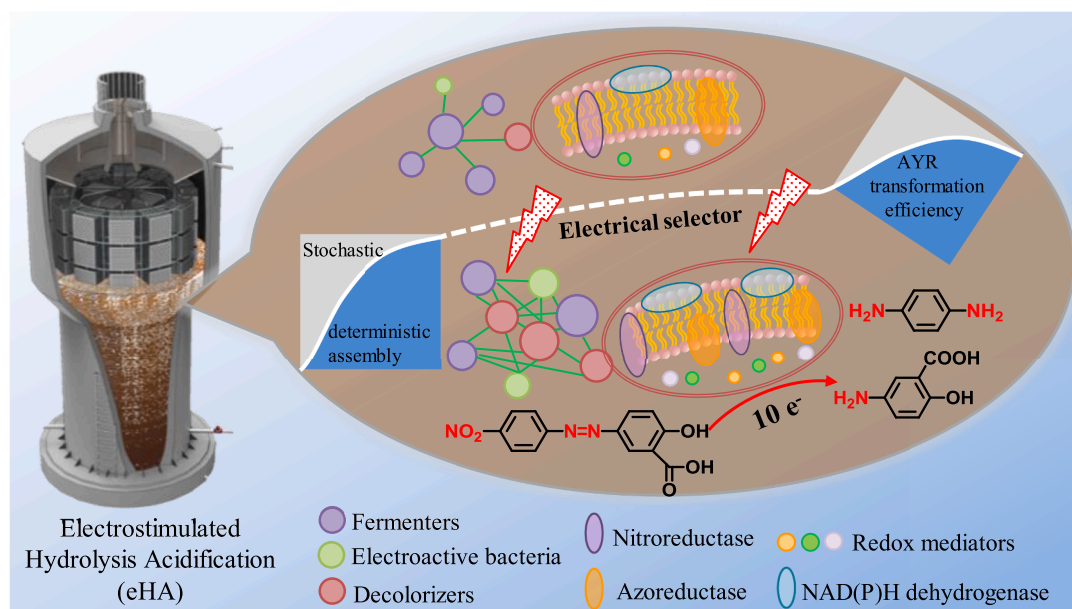


Fig. 7.. Conceptual model of the effect of electrostimulation on planktonic sludge microbial community in the eHA system.

electroselection could be transferred to the HA unit through a bypass backflow, which may also have the effect of improving the functional performance. The proposed electro-regulation strategy is expected to update the technical concept of wastewater anaerobic biological treatment. Furthermore, more systematic and in-depth studies are needed to evaluate the relationship of planktonic sludge and electrode biofilm as well as the effect and mechanism of electrostimulation on microorganisms within the eHA system at the molecular level.

5. Conclusion

Refractory organic nitrogen contaminants (e.g. azo dye AYR) biotransformation could be significantly accelerated with electrostimulation as compared to conventional HA. Electrostimulation significantly altered the planktonic sludge phylogenetic and functional microbial community composition and structure, also, fermenters (e.g. *norank_f_Bacter_vadinHA17*) entered into a greater number of cooperative relationships with decolorizers (e.g. *Acinetobacter*) and electroactive bacteria (e.g. *Desulfobulbus*). Higher abundances of decolorizer (e.g. *Acinetobacter* and *Dechloromonas*) related degradative genes (e.g. azoreductase and nitroreductase) and electroactive bacteria (e.g. *Pseudomonas* and *Desulfobulbus*) related mediator biosynthesis genes (e.g. menaquinone and ubiquinone) were observed in the electrostimulation microcosms. Furthermore, the planktonic sludge microbial community assembly was more driven by deterministic processes upon electrostimulation. This study provides new insights into our understanding of how electrostimulation affects planktonic sludge microbial community function and assembly and improves the biotransformation efficiency of refractory organic nitrogen contaminants in the HA system.

Declaration of Competing Interest

The authors declare that they have no known competing financial interests or personal relationships that could have appeared to influence the work reported in this paper.

Acknowledgments

The study was financially supported by the NSFC-EU Environmental Biotechnology joint program (No. 31861133001), State Key Laboratory of Urban Water Resource and Environment (Harbin Institute of Technology) (No. 2021TS19), Shenzhen Overseas High-level Talents Research Startup Program (FG11409005), and Shenzhen Science and Technology Program (No. KQTD20190929172630447).

Supplementary materials

Supplementary material associated with this article can be found, in the online version, at [doi:10.1016/j.watres.2021.117744](https://doi.org/10.1016/j.watres.2021.117744).

Reference

- Bai, Y., Liang, B., Yun, H., Zhao, Y., Li, Z., Qi, M., Ma, X., Huang, C., Wang, A., 2021. Combined bioaugmentation with electro-biostimulation for improved bioremediation of antimicrobial triclocarban and PAHs complexly contaminated sediments. *J. Hazard. Mater.* 403, 123937.
- Banerjee, S., Walder, F., Buechi, L., Meyer, M., Held, A.Y., Gattinger, A., Keller, T., Charles, R., van der Heijden, M.G.A., 2019. Agricultural intensification reduces microbial network complexity and the abundance of keystone taxa in roots. *ISME J.* 13 (7), 1722–1736.
- Burns, A.R., Stephens, W.Z., Stagaman, K., Wong, S., Rawls, J.F., Guillemin, K., Bohannon, B.J., 2016. Contribution of neutral processes to the assembly of gut microbial communities in the zebrafish over host development. *ISME J.* 10, 655–664.
- Chang, J.S., Chou, C., Lin, Y.C., Lin, P.J., Ho, J.Y., Hu, T.L., 2001. Kinetic characteristics of bacterial azo-dye decolorization by *Pseudomonas luteola*. *Water Res.* 35 (12), 2841–2850.
- Chen, D., Shen, J., Jiang, X., Su, G., Han, W., Sun, X., Li, J., Mu, Y., Wang, L., 2019a. Simultaneous debromination and mineralization of bromophenol in an up-flow electricity-stimulated anaerobic system. *Water Res.* 157, 8–18.
- Chen, F., Li, Z.L., Liang, B., Yang, J.Q., Cheng, H.Y., Huang, C., Nan, J., Wang, A.J., 2019b. Electrostimulated bio-dechlorination of trichloroethene by potential regulation: kinetics, microbial community structure and function. *Chem. Eng. J.* 357, 633–640.
- Chen, Z., Li, D., Wen, Q., 2020. Investigation of hydrolysis acidification process during anaerobic treatment of coal gasification wastewater (CGW): evolution of dissolved organic matter and biotoxicity. *Sci. Total Environ.* 723, 137955.
- Cheng, J., Li, S., Yang, X., Huang, X., Lu, Z., Xu, J., Yu, H., 2021. Regulating the dechlorination and methanogenesis synchronously to achieve a win-win remediation solution for γ -hexachlorocyclohexane polluted anaerobic environment. *Water Res.* 203, 117542.
- Choi, O., Kim, J., Kim, J.G., Jeong, Y., Moon, J.S., 2008. Pyrroloquinoline quinone is a plant growth promotion factor produced by *Pseudomonas fluorescens* B16. *Plant Physiol.* 146 (2), 657–668.
- Cohen, S.G., Wang, C.H., 2002. The effects of structure on the kinetics of decomposition of substituted phenyl-azo-triphenylmethanes. *J. Am. Chem. Soc.* 75 (22), 5504–5507.
- Cui, D., Guo, Y.Q., Lee, H.S., Wu, W.M., Liang, B., Wang, A.J., Cheng, H.Y., 2014. Enhanced decolorization of azo dye in a small pilot-scale anaerobic baffled reactor coupled with biocatalyzed electrolysis system (ABR-BES): a design suitable for scaling-up. *Bioresour. Technol.* 163, 254–261.
- Cui, M.H., Cui, D., Gao, L., Wang, A.J., Cheng, H.Y., 2016a. Azo dye decolorization in an up-flow bioelectrochemical reactor with domestic wastewater as a cost-effective yet highly efficient electron donor source. *Water Res.* 105, 520–526.
- Cui, M.H., Cui, D., Gao, L., Cheng, H.Y., Wang, A.J., 2016b. Efficient azo dye decolorization in a continuous stirred tank reactor (CSTR) with built-in bioelectrochemical system. *Bioresour. Technol.* 218, 1307–1311.
- Dan, C., Guo, Y.Q., Cheng, H.Y., Liang, B., Kong, F.Y., Lee, H.S., Wang, A.J., 2012. Azo dye removal in a membrane-free up-flow biocatalyzed electrolysis reactor coupled with an aerobic bio-contact oxidation reactor. *J. Hazard. Mater.* 239 (240), 257–264.
- De Vrieze, J., Arends, J.B.A., Verbeeck, K., Gildemyn, S., Rabaey, K., 2018. Interfacing anaerobic digestion with (bio) electrochemical systems: potentials and challenges. *Water Res.* 146, 244–255.
- Deng, Y., Jiang, Y.H., Yang, Y., He, Z., Luo, F., Zhou, J., 2012. Molecular ecological network analyses. *BMC Bioinform.* 13, 113.
- Du, Q., Mu, Q., Cheng, T., Li, N., Wang, X., 2018. Real-time imaging revealed that exoelectrogens from wastewater are selected at the center of a gradient electric field. *Environ. Sci. Technol.* 52 (15), 8939–8946.
- Feng, K., Zhang, Z., Cai, W., Liu, W., Xu, M., Yin, H., Wang, A., He, Z., Deng, Y., 2017. Biodiversity and species competition regulate the resilience of microbial biofilm community. *Mol. Ecol.* 26 (21), 6170–6182.
- Guerrero, L., Omil, F., Mendez, R., 1999. Anaerobic hydrolysis and acidogenesis of wastewaters from food industries with high content of organic solids and protein. *Water Res.* 33 (12), 3281–3290.
- Guo, K., Freguia, S., Dennis, P.G., Chen, X., Donose, B.C., Keller, J., Gooding, J.J., Rabaey, K., 2013. Effects of surface charge and hydrophobicity on anodic biofilm formation, community composition, and current generation in bioelectrochemical systems. *Environ. Sci. Technol.* 47 (13), 7563–7570.
- He, Y., Tian, Z., Yi, Q., Zhang, Y., Yang, M., 2020. Impact of oxytetracycline on anaerobic wastewater treatment and mitigation using enhanced hydrolysis pretreatment. *Water Res.* 187 (5), 116408.
- He, Z.W., Yang, C.X., Tang, C.C., Liu, W.Z., Zhou, A.J., Ren, Y.X., Wang, A.J., 2021. Response of anaerobic digestion of waste activated sludge to residual ferric ions. *Bioresour. Technol.* 322, 124536–124536.
- Hirose, A., Kasai, T., Aoki, M., Umemura, T., Watanabe, K., Kouzuma, A., 2018. Electrochemically active bacteria sense electrode potentials for regulating catabolic pathways. *Nat. Commun.* 9, 1083.
- Jiang, X., Shen, J., Xu, K., Chen, D., Mu, Y., Sun, X., Han, W., Li, J., Wang, L., 2018. Substantial enhancement of anaerobic pyridine bio-mineralization by electrical stimulation. *Water Res.* 130, 291–299.
- Katritzky, A.R., Kasemets, K., Slavov, S., Radzivilovits, M., Taemm, K., Karelson, M., 2010. Estimating the toxicities of organic chemicals in activated sludge process. *Water Res.* 44 (8), 2451–2460.
- Kong, D., Liang, B., Yun, H., Cheng, H., Ma, J., Cui, M., Wang, A., Ren, N., 2015. Cathodic degradation of antibiotics: characterization and pathway analysis. *Water Res.* 72, 281–292.
- Kong, F., Ren, H.Y., Pavlostathis, S.G., Wang, A., Nan, J., Ren, N.Q., 2018. Enhanced azo dye decolorization and microbial community analysis in a stacked bioelectrochemical system. *Chem. Eng. J.* 354, 351–362.
- Liang, B., Cheng, H.Y., Kong, D.Y., Gao, S.H., Sun, F., Cui, D., Kong, F.Y., Zhou, A.J., Liu, W.Z., Ren, N.Q., Wu, W.M., Wang, A.J., Lee, D.J., 2013. Accelerated reduction of chlorinated nitroaromatic antibiotic chloramphenicol by biocathode. *Environ. Sci. Technol.* 47 (10), 5353–5361.
- Liang, B., Cheng, H., Van Nostrand, J.D., Ma, J., Yu, H., Kong, D., Liu, W., Ren, N., Wu, L., Wang, A., Lee, D.J., Zhou, J., 2014. Microbial community structure and function of nitrobenzene reduction biocathode in response to carbon source switchover. *Water Res.* 54, 137–148.
- Liang, B., Ma, J., Cai, W., Li, Z., Liu, W., Qi, M., Zhao, Y., Ma, X., Deng, Y., Wang, A., Zhou, J., 2019. Response of chloramphenicol-reducing biocathode resistome to continuous electrical stimulation. *Water Res.* 148, 398–406.
- Liao, C., Wu, J., Zhou, L., Li, T., An, J., Huang, Z., Li, N., Wang, X., 2018. Repeated transfer enriches highly active electrotrophic microbial consortia on biocathodes in microbial fuel cells. *Biosens. Bioelectron.* 121, 118–124.
- Lin, X.Q., Li, Z.L., Liang, B., Zhai, H.L., Cai, W.W., Nan, J., Wang, A.J., 2019. Accelerated microbial reductive dechlorination of 2, 4, 6-trichlorophenol by weak electrical stimulation. *Water Res.* 162, 236–245.

- Liu, G., Zhou, J., Chen, C., Wang, J., Jin, R., Lv, H., 2013. Decolorization of azo dyes by *Geobacter metallireducens*. *Appl. Microbiol. Biotechnol.* 97 (17), 7935–7942.
- Logan, B.E., Rossi, R., Ragab, A.A., Saikaly, P.E., 2019. Electroactive microorganisms in bioelectrochemical systems. *Nat. Rev. Microbiol.* 17 (5), 307–319.
- Long, X., Cao, X., Song, H., Nishimura, O., Li, X., 2019. Characterization of electricity generation and microbial community structure over long-term operation of a microbial fuel cell. *Bioresour. Technol.* 285, 121395.
- Louca, S., Polz, M.F., Mazel, F., Albright, M.B.N., Huber, J.A., O'Connor, M.I., Ackermann, M., Hahn, A.S., Srivastava, D.S., Crowe, S.A., Doebeli, M., Parfrey, L.W., 2018. Function and functional redundancy in microbial systems. *Nat. Ecol. Evol.* 2 (6), 936–943.
- Luo, H., Hu, J., Qu, L., Liu, G., Zhang, R., Lu, Y., Qi, J., Hu, J., Zeng, C., 2019. Efficient reduction of nitrobenzene by sulfate-reducer enriched biocathode in microbial electrolysis cell. *Sci. Total. Environ.* 674, 336–343.
- Luo, J., Chen, Y., Feng, L., 2016. Polycyclic aromatic hydrocarbon affects acetic acid production during anaerobic fermentation of waste activated sludge by altering activity and viability of acetogen. *Environ. Sci. Technol.* 50 (13), 6921.
- Martinez, C.M., Alvarez, L.H., 2018. Application of redox mediators in bioelectrochemical systems. *Biotechnol. Adv.* 36 (5), 1412–1423.
- Miran, W., Nawaz, M., Kadam, A., Shin, S., Heo, J., Jang, J., Lee, D.S., 2015. Microbial community structure in a dual chamber microbial fuel cell fed with brewery waste for azo dye degradation and electricity generation. *Environ. Sci. Pollut. Res.* 22 (17), 13477–13485.
- Ning, D., Deng, Y., Tiedje, J.M., Zhou, J., 2019. A general framework for quantitatively assessing ecological stochasticity. *Proc. Natl. Acad. Sci. U S A.* 116 (34), 16892–16898.
- Ning, D., Yuan, M., Wu, L., Zhang, Y., Guo, X., Zhou, X., Yang, Y., Arkin, A.P., Firestone, M.K., Zhou, J., 2020. A quantitative framework reveals ecological drivers of grassland microbial community assembly in response to warming. *Nat. Commun.* 11 (1), 4717.
- Park, J.G., Jiang, D., Lee, B., Jun, H.B., 2020. Towards the practical application of bioelectrochemical anaerobic digestion (BEAD): insights into electrode materials, reactor configurations, and process designs. *Water Res.* 184, 116214.
- Sarkar, S., Banerjee, A., Halder, U., Biswas, R., Bandopadhyay, R., 2017. Degradation of synthetic azo dyes of textile industry: a sustainable approach using microbial enzymes. *Water Conserv. Sci. Eng.* 2 (4), 121–131.
- Shi, K., Liang, B., Guo, Q., Zhao, Y., Sharif, H.M.A., Li, Z., Chen, E., Wang, A., 2021. Accelerated bioremediation of a complexly contaminated river sediment through ZVI-electrode combined stimulation. *J. Hazard. Mater.* 413, 125392.
- Sloan, W.T., Lunn, M., Woodcock, S., Head, I.M., Nee, S., Curtis, T.P., 2010. Quantifying the roles of immigration and chance in shaping prokaryote community structure. *Environ. Microbiol.* 8 (4), 732–740.
- Wang, A.J., Cheng, H.Y., Liang, B., Ren, N.Q., Cui, D., Lin, N., Kim, B.H., Rabaey, K., 2011. Efficient reduction of nitrobenzene to aniline with a biocatalyzed cathode. *Environ. Sci. Technol.* 45 (23), 10186–10193.
- Wang, A.J., Wang, H.C., Cheng, H.Y., Liang, B., Liu, W.Z., Han, J.L., Zhang, B., Wang, S.S., 2020a. Electrochemistry-stimulated environmental bioremediation: development of applicable modular electrode and system scale-up. *Environ. Eco. Technol.* 3, 100050.
- Wang, B., Liu, W., Zhang, Y., Wang, A., 2020b. Bioenergy recovery from wastewater accelerated by solar power: intermittent electro-driving regulation and capacitive storage in biomass. *Water Res.* 175, 115696.
- Wang, B., Liu, W., Zhang, Y., Wang, A., 2020c. Intermittent electro field regulated mutualistic interspecies electron transfer away from the electrodes for bioenergy recovery from wastewater. *Water Res.* 185, 116238.
- Wang, H.C., Cheng, H.Y., Cui, D., Zhang, B., Wang, S.S., Han, J.L., Su, S.G., Chen, R., Wang, A.J., 2017. Corrugated stainless-steel mesh as a simple engineerable electrode module in bio-electrochemical system: hydrodynamics and the effects on decolorization performance. *J. Hazard. Mater.* 338, 287–295.
- Wang, H.C., Cheng, H.Y., Wang, S.S., Cui, D., Han, J.L., Hu, Y.P., Su, S.G., Wang, A.J., 2016. Efficient treatment of azo dye containing wastewater in a hybrid acidogenic bioreactor stimulated by biocatalyzed electrolysis. *J. Environ. Sci.* 39, 198–207.
- Wang, K., Li, W., Gong, X., Li, X., Liu, W., He, C., Wang, Z., Minh, Q.N., Chen, C.L., Wang, J.Y., 2014. Biological pretreatment of tannery wastewater using a full-scale hydrolysis acidification system. *Int. Biodeterior. Biodegrad.* 95, 41–45.
- Xu, H., Xiao, L., Zheng, S., Zhang, Y., Li, J., Liu, F., 2019. Reductive degradation of chloramphenicol by *Geobacter metallireducens*. *Sci. China Technol. Sci.* 62 (10), 1688–1694.
- Xu, X., Shao, J., Li, M., Gao, K., Jin, J., Zhu, L., 2016. Reductive transformation of *p*-chloronitrobenzene in the upflow anaerobic sludge blanket reactor coupled with microbial electrolysis cell: performance and microbial community. *Bioresour. Technol.* 218, 1037–1045.
- Yanuka-Golub, K., Dubinsky, V., Korenblum, E., Reshef, L., Gophna, U., 2021. Anode surface bioaugmentation enhances deterministic biofilm assembly in microbial fuel cells. *mBio* 12 (2), e03629, 03620.
- Yu, Y.Y., Wang, Y.Z., Fang, Z., Shi, Y.T., Cheng, Q.W., Chen, Y.X., Shi, W., Yong, Y.C., 2020. Single cell electron collectors for highly efficient wiring-up electronic abiotic/biotic interfaces. *Nat. Commun.* 11 (1), 4087.
- Yuan, M.M., Guo, X., Wu, L., Zhang, Y., Xiao, N., Ning, D., Shi, Z., Zhou, X., Wu, L., Yang, Y., Tiedje, J.M., Zhou, J., 2021. Climate warming enhances microbial network complexity and stability. *Nat. Clim. Chang.* 11 (4), 343–348.
- Zhang, X., PrevotEAU, A., Louro, R.O., Paquete, C.M., Rabaey, K., 2018. Periodic polarization of electroactive biofilms increases current density and charge carriers concentration while modifying biofilm structure. *Biosens. Bioelectron.* 121, 183–191.
- Zhang, Z., Deng, Y., Feng, K., Cai, W., Li, S., Yin, H., Xu, M., Ning, D., Qu, Y., 2019. Deterministic assembly and diversity gradient altered the biofilm community performances of bioreactors. *Environ. Sci. Technol.* 53 (3), 1315–1324.
- Zhao, N., Treu, L., Angelidaki, I., Zhang, Y., 2019. Exoelectrogenic anaerobic granular sludge for simultaneous electricity generation and wastewater treatment. *Environ. Sci. Technol.* 53 (20), 12130–12140.
- Zhou, J.Z., Ning, D.L., 2017. Stochastic community assembly: does it matter in microbial ecology? *Microbiol. Mol. Biol. Rev.* 81 (4), e00002, 00017.
- Zhou, J.Z., Liu, W.Z., Deng, Y., Jiang, Y.H., Xue, K., He, Z.L., Nostrand, J.D., Van, W., L. Y., Yang, Y.F., Wang, A.J., 2013. Stochastic assembly leads to alternative communities with distinct functions in a bioreactor microbial community. *mBio* 4 (2), e00584, 00512.
- Zhou, J.Z., Bruns, M.A., Tiedje, J.M., 1996. DNA recovery from soils of diverse composition. *Appl. Environ. Microbiol.* 62 (2), 316–322.
- Zhou, J., Deng, Y., Luo, F., He, Z., Tu, Q., Zhi, X., 2010. Functional molecular ecological networks. *mBio* 1 (4), e00169, 00110.
- Zhou, J., Deng, Y., Luo, F., He, Z., Yang, Y., 2011. Phylogenetic molecular ecological network of soil microbial communities in response to elevated CO₂. *mBio* 2 (4), e00122, 00111.